New Journal of Physics
The open access journal at the forefront of physics

Deutsche Physikalische Gesellschaft DPG IOP Institute of Physics

PAPER • OPEN ACCESS

Nanoscale ion implantation using focussed highly charged ions

To cite this article: Paul Räcke *et al* 2020 *New J. Phys.* **22** 083028

View the article online for updates and enhancements.

You may also like

- EBIS charge breeder for radioactive ion beams at ATLAS
P Ostroumov, S Kondrashev, R Pardo et al.
- Development and applications of electron beam ion source for nanoprocesses
M Sakurai, M Tona, H Watanabe et al.
- Analysis of a possible 20A electron gun and collector design for the RHIC EBIS*
Alexander Pikin, James G Alessi, Edward N Beebe et al.

Recent citations

- Vacancy diffusion and nitrogen-vacancy center formation near the diamond surface
P. Räcke *et al*
- Direct formation of nitrogen-vacancy centers in nitrogen doped diamond along the trajectories of swift heavy ions
Russell E. Lake *et al*
- Quantum computer based on color centers in diamond
Sébastien Pezzagna and Jan Meijer

This content was downloaded from IP address 88.130.56.210 on 26/11/2021 at 09:06

New Journal of Physics
The open access journal at the forefront of physics

Deutsche Physikalische Gesellschaft DPG
IOP Institute of Physics

Published in partnership with: Deutsche Physikalische Gesellschaft and the Institute of Physics

OPEN ACCESS

RECEIVED
17 April 2020

REVISED
8 June 2020

ACCEPTED FOR PUBLICATION
29 June 2020

PUBLISHED
11 August 2020

Original content from this work may be used under the terms of the Creative Commons Attribution 4.0 licence.

Any further distribution of this work must maintain attribution to the author(s) and the title of the work, journal citation and DOI.

PAPER

Nanoscale ion implantation using focussed highly charged ions

Paul Räcke[1,2,4], Ralf Wunderlich[3], Jürgen W Gerlach[1,2], Jan Meijer[2,3] and Daniel Spemann[1,2]

[1] Leibniz Institute of Surface Engineering (IOM), Permoserstr. 15, D-04318 Leipzig, Germany
[2] Leibniz Joint Lab 'Single Ion Implantation', Permoserstr. 15, D-04318 Leipzig, Germany
[3] Felix Bloch Institute for Solid State Physics, Applied Quantum Systems Department, Universität Leipzig, Linnéstr. 5, D-04103 Leipzig, Germany
[4] Author to whom any correspondence should be addressed.

E-mail: paul.raecke@iom-leipzig.de

Keywords: ion implantation, colour centres, nano technology, ion optics, focussed ion beam, electron beam ion source, highly charged ions

Supplementary material for this article is available online

Abstract

We introduce a focussed ion beam (FIB) based ion implanter equipped with an electron beam ion source (EBIS), able to produce highly charged ions. As an example of its utilisation, we demonstrate the direct writing of nitrogen-vacancy centres in diamond using focussed, mask-less irradiation with Ar^{8+} ions with sub-micron three dimensional placement accuracy. The ion optical system was optimised and is characterised via secondary electron imaging. The smallest measured foci are below 200 nm, using objective aperture diameters of 5 and 10 μm, showing that nanoscale ion implantation using an EBIS is feasible.

1. Introduction

Ion implantation is not only an established technique for semiconductor industry and research, but also a key method enabling groundbreaking research in novel quantum technologies, e.g. based on donors in silicon [1–4] or the nitrogen-vacancy-(NV)-centre in diamond [5–10]. One issue for further experimental realisation of quantum computing schemes is the scalability of the qubit fabrication [11]. For ion implantation, this means combining a high throughput and spatially precise placement of single dopants and defects is crucial.

The underlying main motivation for the present work is the development of a deterministic single ion implantation method. Deterministic means that a specified number of single ions are implanted into predetermined positions, which is a key requirement for developing an impurity based solid state quantum computer. For this purpose, it is planned to employ image charge detection for detecting the ions along their trajectory from the ion source to the target (pre-detection) [12–14]. Image charge detection works by amplifying and measuring the image charge created when ions pass through an array of metallic electrodes inside a specially designed image charge detector, which is currently under development [12]. More details can be found in previous publications [12, 13], but the main aspect relevant for the work presented here is that the image charge signal is proportional to the single ion charge state. Electronic noise is a fundamental limitation of the sensitivity of an image charge detector, and it is estimated that highly charged ions are necessary to make this detection scheme feasible [13]. This pre-detection method offers advantages, but also demands that none of the detected ions are lost on their way from the detector to the target. Therefore, a focussed ion beam is used instead of lithographic or other types of masks. Due to these two requirements, focussed ion beam (FIB) technology is used in combination with an electron beam ion source (EBIS), which is capable of producing a variety of multiply to highly charged ions, up to full ionisation [15–18]. Focussing a beam of highly charged ions from an EBIS to a beam spot in the order of 100 nm requires either a beam collimation with very small apertures in the single micrometer range, or a significant enhancement of the demagnification compared to a conventional FIB system using a liquid metal ion

© 2020 The Author(s). Published by IOP Publishing Ltd on behalf of the Institute of Physics and Deutsche Physikalische Gesellschaft

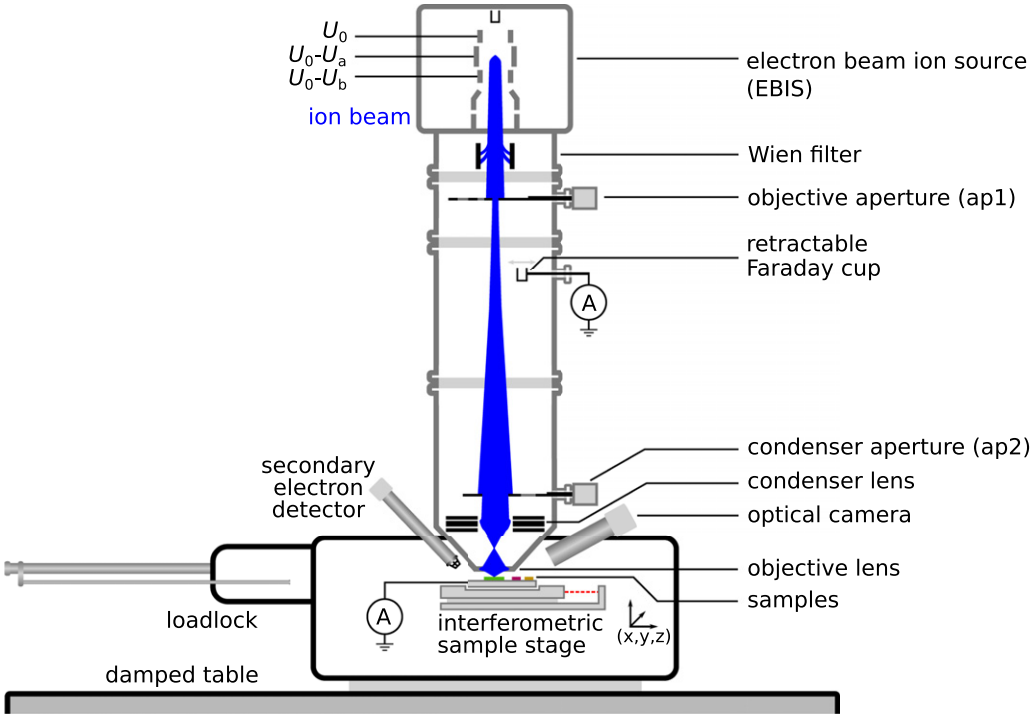

Figure 1. Schematic of the focussed ion beam-based electron beam ion source ion implanter. The beam envelope between objective aperture and sample is based on an actual ray tracing simulation ($U_0 = 12$ kV, Ar^{8+}), confirming the existence of a crossover focus between condenser lens and objective lens for $V_{CL} = 5.0$ kV.

source. So far, a micro-scale beam spot focus from a combined EBIS–FIB system was achieved for noble gas ions [17, 18]. Furthermore, the usage of highly charged ions together with collimating masks near the sample to achieve nano-scale lateral resolution was already proposed for single ion implantation of phosphorous [19, 20] and NV-centre creation [21]. Here, we introduce a set-up with the ability to focus highly charged ions from an EBIS to a beam spot of less than 200 nm. Using the FIB system, arbitrary implantation patterns can be written easily and without the need for lithographic or other types of masking or patterning procedures near the sample surface. In comparison with ion implanters using only singly charged ions, the kinetic energy can easily be changed by selecting different charge states, but keeping all other electrostatic lens settings. Furthermore, high charge states make kinetic energies in the range of several hundred keV accessible, that are typically not available in a compact FIB set-up. We present a characterisation of the ion optical system and, as an example, show the creation of nitrogen-vacancy centre arrays in diamond by localised generation of vacancies induced by Ar^{8+} irradiation. These ions possess a kinetic energy of 96 keV using an accelerating potential of only 12 kV.

2. Experimental methods

The ion implanter at the Leibniz Joint Lab 'Single Ion Implantation' is based on a commercially available Raith ionLINE focussed ion beam (FIB) machine. The gallium liquid metal ion source (LMIS) was replaced by an electron beam ion source (EBIS), which is able to provide highly charged, up to completely ionised species from injected gas [15, 22]. Specific charge states can be selected using a Wien filter. A schematic of the whole set-up is given in figure 1. The drift length between Wien filter and the entrance of the FIB column (i.e. the condenser lens) provides space for beam diagnostics, such as the Faraday cup and the image charge detector that is currently under development [12, 13]. Furthermore, it is ion optically advantageous to have a large ratio of the distances between objective aperture and condenser lens (CL) and objective lens (OL) and focal plane (working distance), respectively. For the experiments presented in this work, argon gas was injected by a PID controlled valve to a pressure of 2.05×10^{-8} hPa. In principle, any gaseous substance can be ionised in the EBIS, however with varying resulting cathode life times [16]. The EBIS was configured with an accelerating voltage of $U_0 = 12$ kV in continuous beam mode, with trap voltages adjusted to yield an optimum current for the desired charge state (see figure 2). To achieve the smallest focus of the beam on the sample surface, the lens voltages are $V_{CL} = 5.000$ kV and $V_{OL} = 7.452$ kV at a working distance of 10 mm. Our measurements and ray tracing simulations show that this condenser

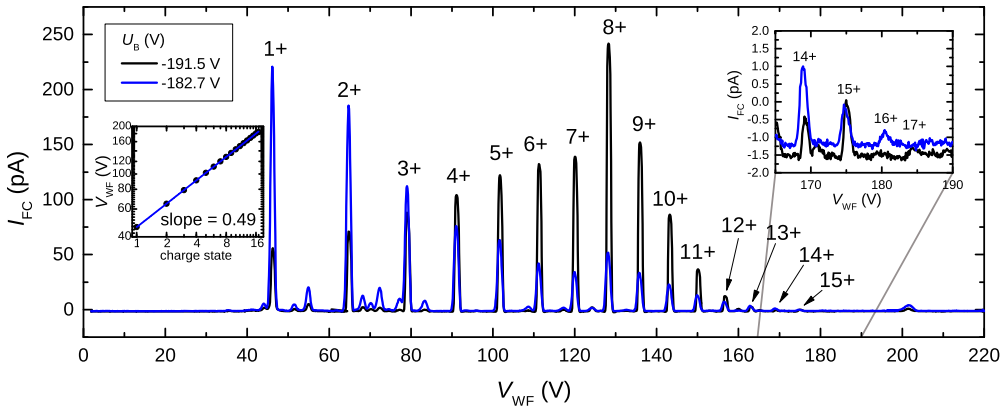

Figure 2. Argon ion beam composition of the EBIS in continuous mode, as measured using a Wien filter voltage sweep for different trap settings to yield more or less highly charged ions. The left inset shows the voltage values as a function of identified Ar charge state lying on a straight line with an apparent slope of 0.5 in double logarithmic scale, confirming correct identification.

lens setting leads to a focus of the beam between the two lenses, which is demagnified a second time by the objective lens. Secondary electrons are registered using an Everhart–Thornley type detector [23]. An electrostatic steering unit below the Wien filter enables optimisation of the beam current in the Faraday cup or on the sample surface. The sample holder itself is mounted electrically insulated from the chamber, enabling direct beam current measurement. The FIB column includes a high speed pattern generator scanning unit and an octupole stigmator for beam shape correction. The apertures are selected and positioned by accurate aperture holder systems. The object aperture limits the beam diameter and is demagnified onto the sample by the lens system, while the condenser aperture mainly limits the beam divergence, reducing the chromatic and spherical aberrations.

3. Results

The EBIS beam composition was measured in continuous beam mode using the Faraday cup connected to a Keithley Picoammeter and sweeping the Wien filter voltage for two different settings of the trap voltage U_b, for $U_a = 171.8$ V (see figure 2). A pulsed mode of operating the EBIS is also available to yield more highly charged ions, up to fully ionised Ar^{18+}, however, for secondary electron images the continuous mode is more useful. The peaks in the Wien filter spectra can be clearly identified, while the settings for the blue curve seems to favour ionisation and acceleration of more rest gas ions, which show up in the smaller peaks between the argon signals.

The beam current was measured while selecting Ar^{8+} with the appropriate Wien filter voltage. The retractable cup can be positioned accurately along an axis transversal to the beam. This was used to capture the beam current profiles shown in figure 3(a). The Faraday cup itself has a diameter of 1 mm, corresponding to the total width of the current profile. By scanning over the two edges, the beam full width at half maximum (FWHM) diameter is estimated, idealising it as a Gaussian beam profile convoluted with a step function at the Faraday cup edge. Together with the optimised maximum current readings obtained for all available objective apertures from 20 to 200 µm diamater (figure 3(b)), it can be assessed that the uncollimated Ar^{8+} beam from the Wien filter has a diameter of around 300 µm. Extrapolating the quadratic fit of the currents underestimates the total beam diameter, due to the beam profile concentrating most intensity in the centre.

A straightforward way to evaluate and optimise the beam spot focus is by generating secondary electron images from scans across a well-defined high contrast edge. Again, assuming a Gaussian beam profile, an error function is fitted to the resulting intensity profile across an edge to determine the FWHM. The commonly used 'chessy' calibration sample provides such edges via checker board-like patterns of 1 µm × 1 µm gold squares on silicon (figure 4). To enhance the signal-to-noise ratio in the resulting images by a high beam current, Ar^{8+} was chosen. For objective aperture diameters between 5 and 200 µm, the beam current on the sample varies from 0.1 to 5 pA, respectively (see supplementary information https://stacks.iop.org/NJP/22/083028/mmedia). Compared to typical FIB applications, this is a low current range. However, targeting for example kHz single ion implantation rates, the required current is on the order of only fA, which will allow to further reduce aperture sizes significantly. Measurements for different charge states on edges of a copper TEM grid (which yields a much higher contrast, but less sharp edges compared

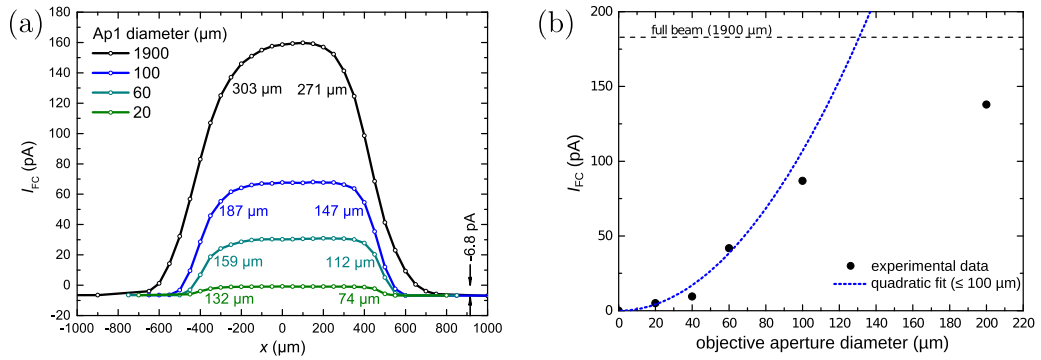

Figure 3. (a) Ar^{8+} ion beam profiles measured at the Faraday cup (between Wien filter and FIB column) for different objective apertures. The lengths aside the graphs give the respective fitted FWHM (b) Ar^{8+} beam current measurements as a function of objective aperture diameter.

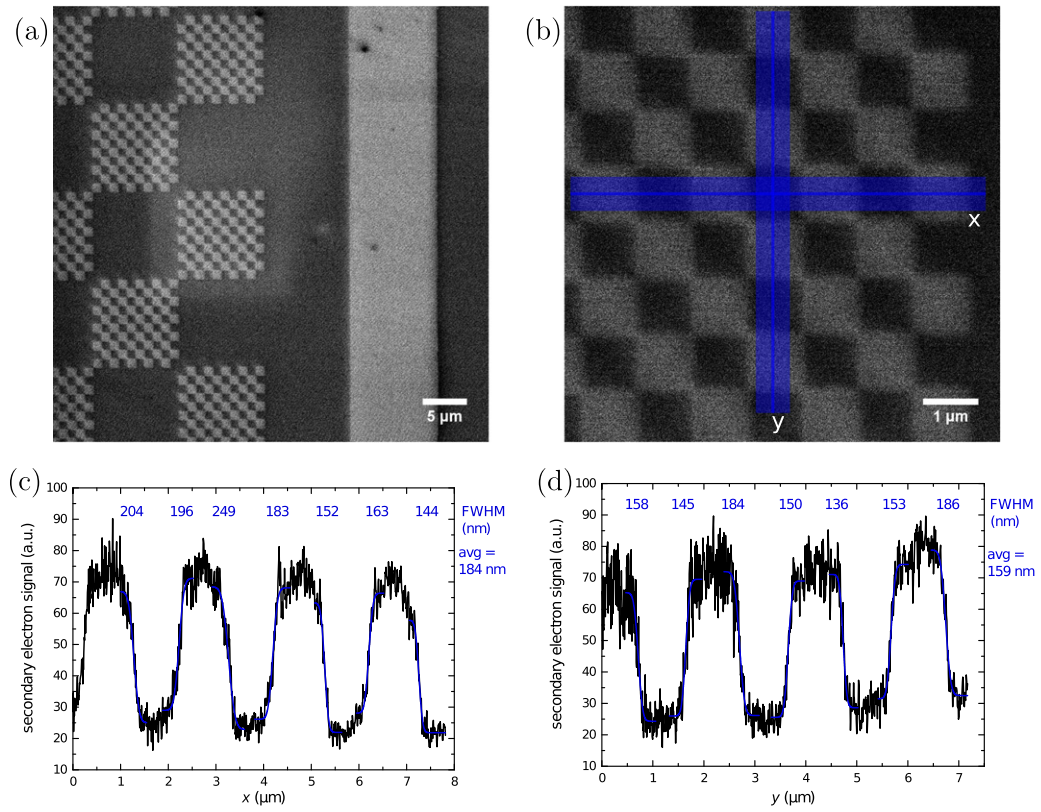

Figure 4. (a) Secondary electron image captured while scanning an Ar^{8+} ion beam (ap1 = 20 µm, ap2 = 20 µm) across a standard chessy calibration sample. (b) Scanning a smaller area, using the same settings, but ap1 = 10 µm. (c) and (d) Plots of line profiles in *x*- and *y*-direction [as indicated in (b)] with edge error function fits.

to the chessy sample) are given in the supplement and indicate that the focus FWHM only varies by a factor of two, with smaller foci for higher charge states at the same U_0. This could be attributed to a smaller chromatic aberration, which is proportional to the relative energy uncertainty $\Delta E_{kin}/E_{kin}$, if the origins for ΔE are dominated by thermodynamics [24]. The images in figures 4(a) and (b) were captured with an optimised beam focus for an objective aperture (ap1) of 20 µm and 10 µm with a condenser aperture of 20 µm. Fitting an error function to the edges as indicated in (b), yields an average FWHM of 184 nm (*x*, (c)) and 159 nm (*y*, (d)). The smallest aperture currently useable has a diameter of 5 µm. The resulting secondary electron image line scans are given in the supplement for completeness. The fits indicate a slightly smaller beam diameter of 179 nm (*x*) and 149 nm (*y*), but the extremely low contrast complicates correct edge fitting. Additionally, unwanted coma effects show up more dominantly as intensity gradients across the squares. This hints to more potential for improvement of the ion optical alignment, backed up by the currently used asymmetrical stigmator settings required to achieve the presented image quality.

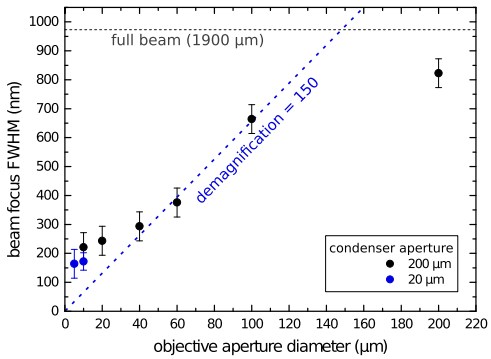

Figure 5. Measurements of the Ar^{8+} ion beam focus FWHM (average of x and y values) from secondary electron images for different aperture configurations.

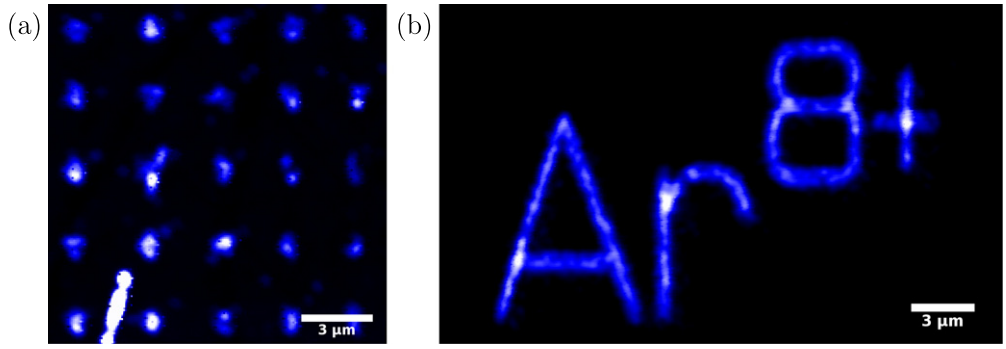

Figure 6. Confocal fluorescence microscopy images of NV-centres created in a diamond sample by local focussed irradiation with Ar^{8+} ions. (a) An array of 5 × 5 spots, with an average fluence of 40 ions per spot. (b) 'Ar^{8+}' written using Ar^{8+} ions. Along each line segment, points with a distance of 5 nm were irradiated with an average of 2 ions each.

A collection of beam spot FWHM values determined from secondary electron images for different aperture settings is shown in figure 5. For apertures >100 µm, the FWHM saturates to the value of the full, uncollimated beam. For lower diameters, there is only a small region between 60 and 100 µm, where the focus size is proportional to the aperture size, i.e. demagnification dominates. The blue dashed diagonal line through the origin indicates a demagnification (as calculated by objective aperture diameter/beam focus FWHM) of 150. At smaller apertures, the FWHM seems to be asymptotically limited for decreasing diameters. This is due to spherical and chromatic aberrations, which are dependent on the beam divergence angle, and can be decreased by choosing a smaller condenser aperture, as it is shown by the two smallest measured foci (blue data points). It is planned to use apertures smaller than 5 µm, however, as discussed, the low resulting beam current makes assessment and optimisation of the ion optical fine-tuning virtually impossible, using secondary electron images only. Instead, low noise single ion detectors, such as an ion beam induced charge (IBIC) sensor should be used [3].

We demonstrate the sub-micron placement of NV-centres in diamond by direct, focussed, mask-less irradiation with highly charged ions. The 5 × 5 spot array and the writing 'Ar^{8+}' shown in figure 6 were produced by local irradiation ($d_{ap1} = 40$ µm, $d_{ap2} = 70$ µm) of a type I diamond sample (100 to 200 ppm nitrogen content) with 96 keV Ar^{8+} ions. A TRIM simulation yields a generation of about 380 vacancies per ion, a lateral straggling of 10 nm and a range ± longitudinal straggling of (51 ± 13) nm [25]. The diamond was annealed for 120 min at 800 °C. Thus, vacancies are allowed to thermally diffuse and the damaged lattice is restored. If a diffusing vacancy encounters a nitrogen impurity atom, it is immobilised by the formation of an NV-centre. The fluorescence of these NV-centres is then recorded in the confocal microscope images. For the parameters of the confocal microscopy measurements please refer to the supplementary information. The differently oriented lines of the written letters in figure 6(b) reveal a slight astigmatism and the presence of coma, as it was concluded from the secondary electron images. Besides intrinsic sample defects, like the scratch in the third quadrant of figure 6(a), the images show localised fluorescence from the intended spot positions. Randomly scattered fluorenscence spots outside the intended positions can be attributed to a background concentration of NV-centres present in the non-irradiated regions of the sample. A histogram of the integrated intensities inside the spots (not shown) is consistent

with a Poisson distribution with a mean value of 20 NV-centres per spot, as calibrated from the integrated intensity of single fluorescent centres found in the non-irradiated areas and lower fluence implantations. Consequently, on average, two implanted argon ions evoked the creation of one NV-centre in this sample. By using a lower average fluence of 4 ions/spot, on average 1.6 NV-centres were created in one spot. Hence, the creation yield per implanted argon ion is constant and single fluorescent centres were created with a probability limited only by fundamental Poisson statistics. A full quantitative characterisation of the mechanism of NV-centre formation from locally placed vacancies is subject of further investigation beyond the scope of this study.

4. Conclusion

In this work, beams of highly charged ions from a focussed ion beam-based ion implanter equipped with an electron beam ion source were characterised and used for the spatially precise creation of arbitrary patterns of nitrogen-vacancy centres. Highly charged ions enable the usage of kinetic energies of multiples of the acceleration potential in a compact set-up by selecting different charge states using a Wien filter, while leaving the lens settings unchanged. The resulting ion energies well in excess of 100 keV offer flexibility and new experimental opportunities not available in conventional FIB systems. Defect engineering in diamond, silicon or other substrates for qubits or spin sensors demands flexibility of the ion species and kinetic energy. Especially for heavier ions, that become more intersting for novel applications, higher kinetic energies are needed for the desired implantation depth. At the same time, high charge states will directly benefit the development of single ion image charge detection, since the sensitivity of an image charge detector is inversely proportional to the single ion charge state. In the presented set-up, the ability to image secondary electron contrast makes ion beam focussing, optimisation and alignment with micro- or nano-markers on samples feasible. A beam spot focus full width at half maximum of less than 200 nm was recorded on a calibration sample using 5 and 10 μm objective aperture diameters. As our results indicate, smaller focal spots should be possible using smaller apertures and further optimisation of the ion optical alignment, then probably requiring single ion detection, such as ion beam induced charge (IBIC) [3] at the sample plane, to image the focal spot with sufficient contrast at reduced beam currents. This work is a milestone on the way to EBIS-based nano-scale ion implantation with highly charged ions, which is crucial for the development of deterministic ion implantation using image charge detection and can be applied to arbitrary substrates and a large variety of implanted ion species. The combination of the high spatial placement fidelity of a FIB system with the versatility of an EBIS is a very promising approach for the scalable production of quantum devices.

Acknowledgments

We gratefully acknowledge the ongoing support and technical assistence of Raith GmbH, Dortmund, Germany, and Dreebit GmbH, Großröhrsdorf, Germany. The authors would like to thank Thomas Pröhl (IOM Leipzig) for his contribution optimising the ion optics. This work is carried out within the Leibniz Joint Lab 'Single Ion Implantation'. We are grateful to receive funding by the Leibniz Association (SAW-2015-IOM-1) and the European Union together with the Sächsisches Ministerium für Wissenschaft und Kunst (Project No. 100308873). JM and RW acknowledge the financial support from the European Union (ASTERIQS, MICROSENS), the BMBF: DiaquantFAB as well as the Deutsche Forschungsgemeinschaft (Ulysses).

ORCID iDs

Paul Räcke https://orcid.org/0000-0002-1229-788X

References

[1] Kane B E 1998 *Nature* **393** 133
[2] van Donkelaar J *et al* 2015 *J. Phys.: Condens. Matter* **27** 154204
[3] Jamieson D N, Lawrie W I, Robson S G, Jakob A M, Johnson B C and McCallum J C 2017 *Mater. Sci. Semicond. Process.* **62** 23–30
[4] Tosi G, Mohiyaddin F A, Schmitt V, Tenberg S, Rahman R, Klimeck G and Morello A 2017 *Nat. Commun.* **8** 2041–1723
[5] Meijer J, Burchard B, Domhan M, Wittmann C, Gaebel T, Popa I, Jelezko F and Wrachtrup J 2005 *Appl. Phys. Lett.* **87** 261909
[6] Pezzagna S, Naydenov B, Jelezko F, Wrachtrup J and Meijer J 2010 *New J. Phys.* **12** 065017
[7] Doherty M W, Manson N B, Delaney P, Jelezko F, Wrachtrup J and Hollenberg L C 2013 *Phys. Rep.* **528** 1–45
[8] Dolde F *et al* 2013 *Nat. Phys.* **9** 139–43

[9] Lesik M et al 2016 Phys. Status Solidi A 213 2594–600
[10] Lühmann T, John R, Wunderlich R, Meijer J and Pezzagna S 2019 Nat. Commun. 10 4956
[11] DiVincenzo D P 2000 Fortschr. Phys. 48 771–83
[12] Räcke P, Spemann D, Gerlach J W, Rauschenbach B and Meijer J 2018 Sci. Rep. 8 9781
[13] Räcke P, Staacke R, Gerlach J W, Meijer J and Spemann D 2019 J. Phys. D: Appl. Phys. 52 305103
[14] Herzig T et al 2018 Creation of quantum centers in silicon using spatial selective ion implantation of high lateral resolution 22nd International Conference on Ion Implantation Technology (IIT) pp 136–9
[15] Zschornack G, Grossmann F, Kentsch U, Ovsyannikov V P, Ritter E, Schmidt M, Thorn A and Ullmann F 2010 Rev. Sci. Instrum. 81 02A512
[16] Ullmann F 2006 Untersuchung der erzeugung hochgeladener ionen in einer raum-temperatur-elektronenstrahl-ionenfalle PhD Thesis Technische Universität Dresden
[17] Ullmann F, Grossmann F, Ovsyannikov V P, Gierak J, Bourhis E, Ferré J, Jamet J P, Mougin A and Zschornack G 2007 J. Vac. Sci. Technol. B 25 2162–7
[18] Schmidt M, Laux P F, Gierak J and Zschornack G 2018 AIP Conf. Proc. 2011 090027
[19] Schenkel T et al 2003 J. Appl. Phys. 94 7017–24
[20] Schenkel T, Weis C D, Lo C C, Persaud A, Chakarov I, Schneider D H and Bokor J 2015 AIP Conf. Proc. 1640 124–8
[21] Tona M and Takahashi S 2004 J. Phys.: Conf. Ser. 2 57–64
[22] Schmidt M, Peng H, Zschornack G and Sykora S 2009 Rev. Sci. Instrum. 80 063301
[23] Everhart T E and Thornley R F M 1960 J. Sci. Instrum. 37 246–8
[24] Glaser W 1952 Grundlagen Der Elektronenoptik 1st edn (Berlin: Springer)
[25] Ziegler J F and Biersack J P 2013 The stopping and range of ions in matter SRIM (version 2013) www.srim.org